Contribution from the Departments of Chemistry and Environmental Sciences and Engineering, The University of North Carolina, Chapel Hill, North Carolina 27514, and the Department of Chemistry, University of Arizona, Tucson, Arizona 85721

Effect of Meso Substituents on Exchange-Coupling Interactions in μ-Oxo Iron(III) Porphyrin Dimers

Jeffrey H. Helms, Leonard W. ter Haar, William E. Hatfield,* David L. Harris, K. Jayaraj, Glen E. Toney, Avram Gold,* Tabitha D. Mewborn, and Jeanne R. Pemberton*

Received September 26, 1985

The μ-oxo iron(III) porphyrin dimers $[(TPP)Fe]_2O$, $[(TPP(4\text{-}OCH_3))Fe]_2O$, $[(TPP(4\text{-}CF_3))Fe]_2O$, and $[(TPP(F_5))Fe]_2O$ (where TPP is *meso*-tetraphenylporphyrin, $TPP(4\text{-}OCH_3)$ is *meso*-tetrakis(4-methoxyphenyl)porphyrin, $TPP(4\text{-}CF_3)$ is *meso*-tetrakis-(4-(trifluoromethyl)phenyl)porphyrin, and $TPP(F_5)$ is *meso*-tetrakis(pentafluorophenyl)porphyrin) have been studied to determine the effect of peripheral substituents on the porphyrin rings on properties of the molecules. Variable-temperature magnetic susceptibility studies on solid samples yielded the following exchange-coupling constants for the antiferromagnetically coupled iron(III) ions: $-146.8\ cm^{-1}$, $[(TPP(4\text{-}OCH_3))Fe]_2O$; $-135.7\ cm^{-1}$, $[(TPP)Fe]_2O$; $-136.4\ cm^{-1}$, $[(TPP(4\text{-}CF_3))Fe]_2O$; $-146.9\ cm^{-1}$, $[(TPP(F_5))Fe]_2O$. Variable-temperature ^{13}C NMR studies of dichloromethane solutions yield exchange-coupling constants of $-150\ cm^{-1}$ for $[(TPP(4\text{-}OCH_3))Fe]_2O$, $-145\ cm^{-1}$ for $[(TPP)Fe]_2O$, and $-129\ cm^{-1}$ for $[(TPP(F_5))Fe]_2O$. Raman spectra were collected in the region of the energy of the outer-ring stretching modes found at approximately $1560\ cm^{-1}$. The position of this band is empirically related to the porphyrin core size, and the data indicate that the porphyrin center–pyrrole nitrogen (C_t–N) distances increase in the order $[(TPP(F_5))Fe]_2O < [(TPP(4\text{-}CF_3))Fe]_2O < [(TPP)Fe]_2O < [(TPP(4\text{-}OCH_3))Fe]_2O$. The data support the hypothesis that the porphyrin ring core size increases as the electron-releasing capability of the peripheral substituent increases. For the para-substituted complexes, increasing core size correlates with stronger axial binding, reflected in stronger antiferromagnetic coupling. The anomalous behavior of $[(TPP(F_5))Fe]_2O$ may result from distortions caused by steric interactions of the *o*-fluorines.

Introduction

Although peripheral substituents have been shown to influence redox potentials of iron porphyrins,[1,2] effects on electronic structure and bonding have not been documented systematically. Growing interest in the correlation of porphyrin substitution with physicochemical characteristics is evident in several recent studies[3-6] that have modeled the effects of protein environment on heme properties in hemoproteins by varying the meso aryl substituents of (porphinato)iron(III) complexes. In an extension of work in this important area, we have documented that the $S = {}^3/_2, {}^5/_2$ quantum-mechanical spin admixture of the (perchlorato)(tetraphenylporphinato)iron(III) complexes can be modulated by substitution of the phenyl rings with groups of varying electron-withdrawing/electron-releasing capabilities.[7] The basis for the observed behavior was speculated to lie in changes in iron orbital occupancy brought about by interactions with electron density on the pyrrole nitrogens in the porphyrin molecular orbitals.

In high-spin complexes, such interactions should be reflected in changes in porphyrin core size and iron–axial ligand bond lengths. Antiferromagnetic coupling between high-spin iron centers in μ-oxo dimers[8] should be a suitable probe for detecting the postulated changes. By enhancing electron density in the porphyrin molecular orbitals, which have considerable spin density on the pyrrole nitrogens, electron-releasing meso aryl groups should enhance iron–porphyrin interactions. The consequent porphyrin core expansion and concomitant decrease in the iron–axial oxygen bond length should enhance antiferromagnetic coupling. Hence, $|J|$ is expected to increase with increasing electron-donating capability of the meso substituents. We have prepared and characterized μ-oxo-bridged iron(III) porphyrin dimers with electron-withdrawing/electron-releasing substituents in the meso position in order to test this hypothesis experimentally.

Experimental Section

Synthesis. The μ-oxo dimers, $[(TPP)Fe]_2O$, $[(TPP(4\text{-}OCH_3))Fe]_2O$, $[(TPP(4\text{-}CF_3))Fe]_2O$, and $[(TPP(F_5))Fe]_2O$ (where TPP is *meso*-tetraphenylporphyrin, $TPP(4\text{-}OCH_3)$ is *meso*-tetrakis(4-methoxyphenyl)-porphyrin, $TPP(4\text{-}CF_3)$ is *meso*-tetrakis(4-(trifluoromethyl)phenyl)-porphyrin, and $TPP(F_5)$ is *meso*-tetrakis(pentafluorophenyl)porphyrin), were prepared from the corresponding chloro complexes by stirring a methylene chloride solution of the chloro(porphinato)iron with an equal volume of aqueous 2 N sodium hydroxide for 4 h. The organic layer was separated, dried over Na_2SO_4, and taken to dryness on a rotary evaporator. The crude solid was purified by chromatography over neutral alumina with benzene or toluene eluent. Fractions containing the μ-oxo dimer were combined and concentrated on a rotary evaporator, and the crystalline dimer was precipitated by addition of hexane. The solid was collected on a fritted filter and transferred to storage vials by a glass spatula. The μ-oxo dimers were evacuated for 2 h at ambient temperature before use in magnetic susceptibility experiments. The following compounds were prepared.

$[(TPP)Fe]_2O$. λ_{max} (toluene) ($\epsilon \times 10^{-3}$, $M^{-1}\ cm^{-1}$): 407 (101), 570 (9.33), 610 (4.66) nm.

Anal. Calcd for $C_{88}H_{56}N_8OFe_2$: C, 78.11, H, 4.14; N, 8.28; Fe, 8.28. Found: C, 78.09; H, 4.29; N, 8.00; Fe, 7.61.

$[(TPP(4\text{-}OCH_3))Fe]_2O$. λ_{max} (toluene) ($\epsilon \times 10^{-3}$, $M^{-1}\ cm^{-1}$): 409 (107), 571 (10.2), 612 (7.0) nm.

Anal. Calcd for $C_{96}H_{72}N_8O_9Fe_2$: C, 72.36; H, 4.52; N, 7.04; Fe, 7.04. Found: C, 72.50; H, 4.73; N, 7.18; Fe, 6.54.

$[(TPP(4\text{-}CF_3))Fe]_2O$. λ_{max} (xylene) ($\epsilon \times 10^{-3}$, $M^{-1}\ cm^{-1}$): 406 (107), 569 (13.6), 610 (3.95) nm.

Anal. Calcd for $C_{96}H_{48}N_8F_{24}OFe_2$: C, 60.76; H, 2.53; N, 5.91; Fe, 5.91. Found: C, 61.61; H, 2.94; N, 5.95; Fe, 5.59.

$[(TPP(F_5))Fe]_2O$. λ_{max} (toluene) ($\epsilon \times 10^{-3}$, $M^{-1}\ cm^{-1}$): 393 (62.4), 557 (7.0), 590 sh (4.6) nm.

Anal. Calcd for $C_{88}H_{16}N_8F_{40}Fe_2O$: C, 50.97; H, 0.77; N, 5.41; Fe, 5.41. Found: C, 51.58; H, 1.47; N, 5.36; Fe, 5.00.

With the exception of the pentafluorophenyl-substituted dimer, the solubilities of the dimers in toluene and benzene were low and the chromatography was inconvenient. However the standard procedure utilizing chloroform[9] or methylene chloride as eluant invariably resulted in the presence of trace quantities of high-spin contaminants, even with rigorously purified chlorocarbon solvents.

Magnetic Susceptibility Measurements. Magnetic susceptibility data were collected by using a computer-controlled Faraday balance consisting

* To whom correspondence should be addressed: W.E.H., Department of Chemistry, The University of North Carolina; A.G., Department of Environmental Sciences and Engineering, The University of North Carolina; J.E.P., University of Arizona.

(1) Kadish, K. M.; Morrison, M. M. *Bioinorg. Chem.* **1977**, *7*, 107.
(2) Walker, F. A.; Beroiz, D.; Kadish, K. M. *J. Am. Chem. Soc.* **1976**, *98*, 3484.
(3) Walker, F. A.; Balke, V. L.; McDermott, G. A. *J. Am. Chem. Soc.* **1982**, *104*, 1569.
(4) Walker, F. A.; Balke, V. L.; McDermott, G. A. *Inorg. Chem.* **1982**, *21*, 3342.
(5) Geiger, D. K.; Scheidt, W. R. *Inorg. Chem.* **1984**, *23*, 1970.
(6) Scheidt, W. R.; Lee, J. Y.; Geiger, D. K.; Taylor, K.; Hatano, K. *J. Am. Chem. Soc.* **1982**, *104*, 3367.
(7) Toney, G. E.; Gold, A.; Savrin, J.; ter Haar, L. W.; Sangaiah, R.; Hatfield, W. E. *Inorg. Chem.* **1984**, *23*, 4350.
(8) For a review, see: Murray, K. S. *Coord. Chem. Rev.* **1974**, *12*, 1.
(9) Adler, A. D.; Longo, F. R.; Varadi, V. *Inorg. Synth.* **1976**, *16*, 213.

0020-1669/86/1325-2334$01.50/0

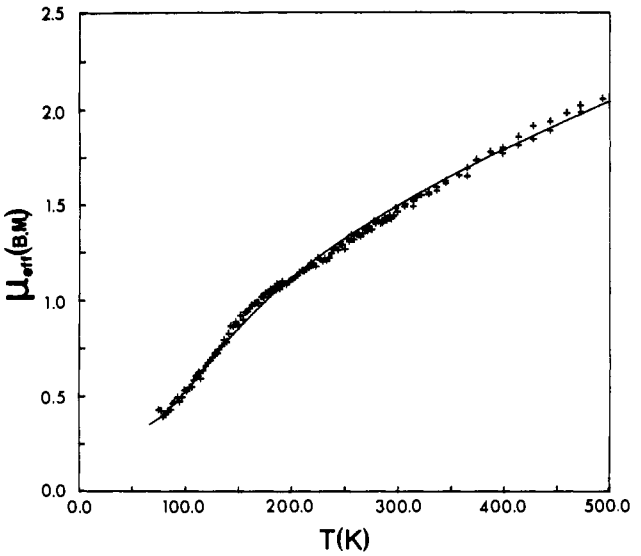

Figure 1. Variable-temperature magnetic moment data for $[(TPP(4\text{-}OCH_3))Fe]_2O$.

of Cahn 2000 electrobalance and an ANAC 4-in. electromagnet equipped with Lewis coils[10] and a bipolar current-regulated power supply from George Associates, Berkeley, CA. A Tektronix 4052A computer and Hewlett-Packard 3495A scanner with relay actuator were used for the automated data collection.

Samples were contained in a hemispherical quartz sample bucket (7.5-mm diameter) that was suspended by a Pyrex fiber and gold chain. The electrobalance and sample were contained in a closed glass system, which was evacuated and filled with helium gas before measurements were made.

Variable temperatures were obtained by surrounding the sample zone with a Dewar flask containing liquid nitrogen. The liquid nitrogen was allowed to evaporate, and the temperature in the system increased gradually as the level of the liquid decreased in the Dewar. A single set of measurements from 77 K to room temperature required approximately 10 h. Sample temperatures were measured with a calibrated gallium arsenide diode and a Fluke 8502A 6.5-place voltmeter. The gallium arsenide diode was placed in the sample zone within 2–3 mm from the sample bucket. The Faraday balance was calibrated with $HgCo(NCS)_4$,[11] and diamagnetic corrections for the constituent atoms were made by using Pascal's constants.[12]

^{13}C NMR Spectra. ^{13}C NMR spectra of the paramagnetic complexes were obtained by using a Bruker WM250 NMR spectrometer operating at 62.896 MHz with a pulse width of 10 μs (75°; 5-mm sample tubes) and 21 μs (72°; 10-mm sample tubes). In the spectral collection, 2048 data points were collected in about 1 h at each temperature. The time between pulses was 32.8 ms. Sample concentrations were approximately 2 mM. The temperatures were measured with a thermocouple that had been calibrated previously with 100% methanol proton chemical shifts. The thermocouple was located 1 mm below the sample tube. The chemical shifts were measured relative to the solvent CD_2Cl_2 ^{13}C signal at 53.8 ppm. Broadband ^1H decoupling was used in all experiments. Free bases were used to obtain diamagnetic reference shifts for pyrrole α- and β-carbons. Shifts of $TPPH_2$ differed from those reported for the scandium μ-oxo dimer[13] by less than 1 ppm, and the close correspondence was assumed to hold for the other compounds. The ^{13}C spectra of diamagnetic samples were obtained in 15-h runs using 22° pulses, 16K data points, and 0.52 s between pulses.

Raman Spectroscopy. The Raman system used for these experiments consisted of a Spex 1403 double monochromator with 1800 grooves/mm holographically ruled gratings. A GaAs photocathode and RCA C31034 photomultiplier tube, which was thermoelectrically cooled to −25 °C, served as the detection system. The excitation wavelength was the 5145-Å line from a Coherent Radiation Innova 90-5 argon ion laser. Spectral points were taken at 0.25-cm^{-1} increments over a 1-s integration time. All spectra are the result of signal averaging of 3–5 scans. A spectral bandpass of 4 cm^{-1} (400 μm) was used to collect all spectra. The data were subsequently subjected to a 5- or 9-point Savitzky–Golay smoothing routine.[14] The monochromator was calibrated at 1483 cm^{-1} by using the 5570.45-Å line of the molybdenum hollow-cathode lamp.

The iron porphyrin samples were dissolved in approximately millimolar concentration in reagent grade CH_2Cl_2 and were analyzed within 2 h of dissolution to prevent degradation. Glass capillaries were used as the sample holder, and the laser power at the sample was ca. 100 mW.

Table I. Magnetic Parameters for the μ-Oxo Iron(III) Porphyrin Dimers

compd	J, cm^{-1}	P
$[(TPP(4\text{-}OCH_3))FeO]_2O$	−146.8 ± 1.1	0.33 ± 0.04
$[(TPP)Fe]_2O$	−135.7 ± 0.3	0.38 ± 0.01
$[(TPP(4\text{-}CF_3))Fe]_2O$	−136.4 ± 1.4	0.64 ± 0.06
$[(TPP(F_5))Fe]_2O$	−146.9 ± 1.4	0.28 ± 0.04

Results

Magnetic Data and Exchange Coupling. The temperature variation of the magnetic moment of $[(TPP(4\text{-}OCH_3))Fe]_2O$ is shown in Figure 1. These data, which reflect antiferromagnetic exchange coupling, are typical of the data in Figures S1–S3 of the supplementary material, which were obtained for the other compounds. The Hamiltonian $H = -2J\hat{S}_1\cdot\hat{S}_2$ was used in the analysis of the data. The solid line in the figure is the best fit to the data of the equation

$$\mu_{eff} = 2.828(\chi_M T)^{1/2}$$

where the magnetic susceptibility χ_M per ion for a pair of exchange-coupled $S = {}^5/_2$ ions is given by

$$\chi_M = (Ng^2\mu_B{}^2/kT)\{\exp(2J/kT) + 5.0\exp(6J/kT) + 14.0\exp(12J/kT) + 30.0\exp(20J/kT) + 55.0\times\exp(30J/kT)\}/\{1 + 3.0\exp(2J/kT) + 5.0\exp(6J/kT) + 7.0\exp(12J/kT) + 9.0\exp(20J/kT) + 11.0\exp(30J/kT)\}$$

Acquisition of acceptable data necessitated magnetic susceptibility experiments on several successively purified samples of each compound. This requirement arose from the presence of an impurity whose magnetic properties obscured the magnetic susceptibility of the μ-oxo iron porphyrin dimers below approximately 200 K. The effect of the impurity on the observed magnetic susceptibility was accounted for by assuming that

$$\chi_{obsd} = \chi_{dimer}/2 + \chi_{impurity}$$

On the additional assumption that the impurity obeys the Curie law, the following expression for the total magnetic susceptibility results:

$$\chi_m = \frac{PNg^2\beta^2S(S+1)}{3kT} + (100 - P)\chi_{dimer}/2$$

where P = the percent impurity and the g value was held constant at 2.0 in all of the calculations. The best-fit parameters and their standard deviations[15] were obtained by using a Simplex nonlinear least-squares program[16,17] as well as the least-squares program in the SAS system[18] with the minimum value of the following function as the criterion of best fit:

$$F = \sum_i \frac{(\chi_i^{obsd} - \chi_i^{calcd})^2}{(\chi_i^{obsd})^2}$$

The best-fit values for J and P for each of the compounds are given in Table I.

(10) Lewis, R. T. *Rev. Sci. Instrum.* **1971**, *42*, 31.
(11) (a) Figgis, B. N.; Nyholm, R. W. *J. Chem. Soc.* **1958**, 4190. (b) Brown, D. B.; Crawford, V. H.; Hall, J. W.; Hatfield, W. E. *J. Phys. Chem.* **1977**, *81*, 1303.
(12) Weller, R. R.; Hatfield, W. E. *J. Chem. Educ.* **1979**, *56*, 652.
(13) Boersma, A. D.; Phillippi, M. A.; Goff, H. M. *J. Magn. Reson.* **1984**, *57*, 197.
(14) Savitzky, A.; Golay, J. J. E. *Anal. Chem.* **1964**, *36*, 1627.
(15) Brown, B. W., Jr.; Hollander, M. *Statistics, A Biomedical Introduction*; Wiley: New York, 1977.
(16) O'Neil, R. *Appl. Stat.* **1971**, *20*, 338.
(17) Nelder, J. A.; Mead, R. *Comput. J.* **1965**, *7*, 308.
(18) *SAS User's Guide: Statistics*, Version 5; SAS Institute Inc.: Cary, NC; 1985.

Table II. Magnetic Parameters for the μ-Oxo Iron(III) Porphyrins from Carbon-13 NMR Studies

compd	^{13}C resonance	J, cm^{-1}	A_1, MHz	A_2, MHz	diamag ref,[a] ppm
$[(TPP(4\text{-}OCH_3))Fe]_2O$	α-pyrrole	−150.0 ± 0.1	0.64	0.72	147
	β-pyrrole		0.59	0.65	131
$[(TPP)Fe]_2O$	α-pyrrole	−145.0 ± 0.2	0.65	0.60	148
	β-pyrrole		0.59	0.57	131
$[(TPP(F_5))Fe]_2O$	α-pyrrole	−128.0 ± 0.2	0.55	0.62	148
	β-pyrrole		0.48	0.56	132

[a] Relative to the free porphyrin base.

^{13}C NMR Results. Temperature-dependent carbon-13 chemical shifts have been reported for $[(TPP)Fe]_2O$ by Goff and co-workers,[13] who deduced the antiferromagnetic exchange-coupling constant from the paramagnetic ^{13}C chemical shifts in agreement with earlier work on proton shifts.[19,20] In order to confirm that any trend in the exchange-coupling constants deduced from the solid-state magnetic susceptibility measurements was a molecular property and not a solid-state effect, we have reproduced the temperature-dependent carbon-13 chemical shifts for $[(TPP)Fe]_2O$ and collected additional temperature-dependent carbon-13 chemical shift data for $[(TPP(4\text{-}OCH_3))Fe]_2O$ and $[(TPP(F_5))Fe]_2O$ (the solubility of $[(TPP(4\text{-}CF_3))Fe]_2O$ was too low for natural-abundance ^{13}C NMR). The data for both compounds are tabulated in Table SI (supplementary material) and are presented in Figure 2.

With the neglect of dipolar shifts, the chemical shift (δ_{obsd}) is given by[13,19-21]

$$\delta_{obsd} = (K/T)\sum A_i\chi_i + \delta_{dia}$$

where

$$K = |\gamma_e|/(3k|\gamma_c|) = 4.18 \times 10^{-8}\ \text{K Hz}^{-1}$$

and

$$\chi_i = \frac{S_i(S_i + 1)n_i \exp(\epsilon_i/kT)}{\sum n_i \exp(\epsilon_i/kT)}$$

The A_i values are electron–nuclear coupling constants for the spin states S_i of the exchnage-coupled cluster. Each spin state (S_i = 0–5) has a multiplicity of $2S_i + 1$ and lies at energy $\epsilon_i = -J[S_i(S_i + 1)]$. Since these systems have J values on the order of −150 cm^{-1}, the states S_i = 3–5 are not populated, and the variables of the problem are therefore J, A_1, and A_2 where the diamagnetic reference δ_{dia} is taken from the spectrum of the corresponding free bases. The expression for δ_{obsd} was fit to the δ_{obsd} data for each μ-oxo dimer by using a Simplex nonlinear least-squares fitting procedure, and the best-fit values for J, A_1, and A_2 for $[(TPP)Fe]_2O$, $[(TPP(4\text{-}OCH_3))Fe]_2O$, and $[(TPP(F_5))Fe]_2O$ are given in Table II. A noteworthy decrease in $|J|$ for $[(TPP(F_5))Fe]_2O$ is evident in the data in Table II. There is generally good agreement of the magnetic parameters for $[(TPP)Fe]_2O$ in Table II with those reported by Goff and co-workers,[13] although a different fitting procedure was used here. In this work, only one exchange-coupling constant was obtained from the best-fit least-squares calculation for the combined α-pyrrole and β-pyrrole ^{13}C chemical shift data for a given μ-oxo dimer, while in the earlier work one best-fit exchange-coupling constant was obtained from the α-pyrrole chemical shifts and a second best-fit J was obtained from the β-pyrrole chemical shifts.

Raman Spectroscopy. The effect of the electron-withdrawing/electron-releasing capability of the meso substituent on core geometry was examined by Raman spectroscopy. The spectra of the μ-oxo iron(III) porphyrin dimers in CH_2Cl_2 in the frequency region between 1530 and 1585 cm^{-1} are presented in Figure 3. The vibrational feature observed at ca. 1560 cm^{-1} in this region has been associated previously with the stretching of the porphyrin outer-ring bonds.[22] Stong and co-workers have shown that the frequency of this band can be correlated with the porphyrin core size, C_t–N (the porphyrin center–pyrrole nitrogen distance in Å), according to the following equation:[23]

$$\nu\ (\text{in cm}^{-1}) = 262.5[7.95 - (C_t\text{–}N)]$$

The peak positions of the four μ-oxo iron(III) porphyrin dimers are summarized in Table III along with the porphyrin center–pyrrole nitrogen distances (in Å) which were calculated from the spectroscopic data. A contraction of 0.05 Å is observed in going

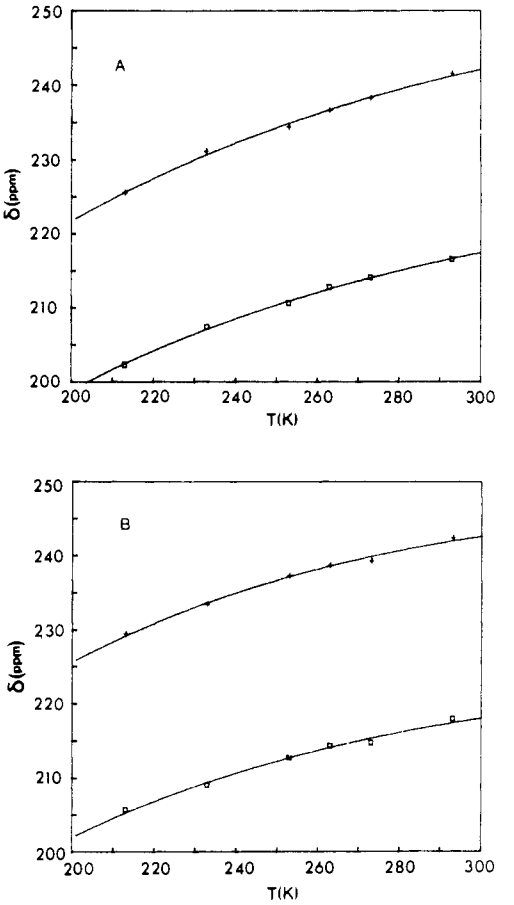

Figure 2. Variable-temperature carbon-13 chemical shift data for the α- and β-pyrrole carbon atoms in (A) $[(TPP(4\text{-}OCH_3))Fe]_2O$ and (B) $[(TPP(F_5))Fe]_2O$. The solid lines are the best least-squares fit to the data as described in the text.

Table III. Band Frequencies and Porphyrin Center–Pyrrole Nitrogen Distances in the μ-Oxo Iron(III) Porphyrins

compd	ν, cm^{-1}	C_t–N, Å
$[(TPP(4\text{-}OCH_3))Fe]_2O$	1552 ± 1	2.04
$[(TPP)Fe]_2O$	1554 ± 1	2.03
$[(TPP(4\text{-}CF_3))Fe]_2O$	1557 ± 1	2.02
$[(TPP(F_5))Fe]_2O$	1564 ± 1	1.99

(19) Boyd, P. D. W.; Smith, T. D. *Inorg. Chem.* **1971**, *10*, 2041.
(20) Wicholas, M.; Mustacich, R.; Jayne, D. *J. Am. Chem. Soc.* **1972**, *94*, 4518.
(21) La Mar, G. N.; Eaton, G. R.; Holm, R. H.; Walker, F. A. *J. Am. Chem. Soc.* **1973**, *95*, 63.
(22) Stein, P.; Ulman, A.; Spiro, T. G. *J. Phys. Chem.* **1964**, *88*, 369.
(23) Stong, J. D.; Spiro, T. G.; Kubaska, R. J.; Shupack, S. I. *J. Raman Spectrosc.* **1980**, *9*, 314.

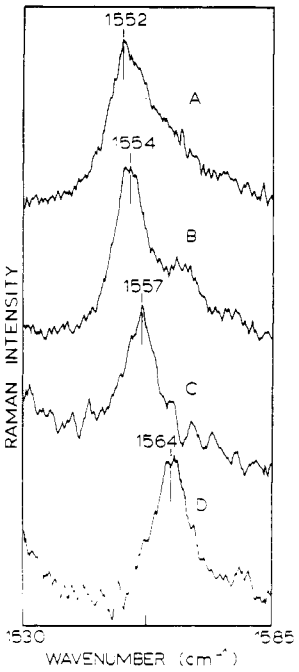

Figure 3. Raman spectra in the region 1530–1585 cm^{-1} of the (μ-oxo)-iron(III) porphyrin dimers in CH_2Cl_2: (A) $[(TPP(4\text{-}OCH_3))Fe]_2O$; (B) $[(TPP)Fe]_2O$; (C) $[(TPP(4\text{-}CF_3))Fe]_2O$; (D) $[(TPP(F_5))Fe]_2O$.

from the electron-donating substituent, $-OCH_3$, to the electron-withdrawing substituent, pentafluorophenyl. The C_t–N distance (2.03 Å) calculated for $[(TPP)Fe]_2O$ on the basis of the Raman frequency is identical with the distance of 2.027 Å reported in the crystal structure.[24]

Discussion

It was postulated that electron-donating/electron-withdrawing substituents on the meso positions of porphyrin rings should influence the core size of the porphyrin ring and that the axial coordination positions of metal ions in the metalloporphyrins would reflect this core size by becoming more acidic, in the Lewis sense, as the core size increases. It was further postulated that this greater attraction for axial ligands should result in enhanced exchange coupling in μ-oxo iron porphyrin dimers and that $|J|$ should increase as the electron-donating ability of the substituent increased.

Magnetic susceptibility data for powder samples of dimers with para-substituted phenyl groups yield exchange-coupling constants that are consistent with the postulates, although the range of values of the exchange-coupling constants is small. The exchange-coupling constants derived from the temperature-dependent carbon-13 NMR chemical shift data for $[(TPP(4\text{-}OCH_3))Fe]_2O$ and $[(TPP)Fe]_2O$ (Table II) are slightly larger than those obtained from the solid-state samples but maintain the same relative ordering, differing by 5 cm^{-1}. The effect is significant since the ^{13}C chemical shift values for $[(TPP(4\text{-}OCH_3))Fe]_2O$ are smaller than those of $[(TPP)Fe]_2O$, as expected from the powerful electron-donating ability of the 4-methoxy substituent. The chemical shift values are very accurate measurements of the relative magnetic susceptibilities of the compounds.

In the absence of exact determination by X-ray crystallographic structural studies, the core size of the porphyrin rings was estimated by monitoring the band at 1560 cm^{-1} in the Raman spectra. The empirical relationship indicates that the cores contract in the order $[(TPP(4\text{-}CF_3))Fe]_2O > [(TPP)Fe]_2O > [(TPP(4\text{-}OCH_3))Fe]_2O$, providing additional support for the influence of peripheral substituents on the Lewis basicity of the pyrrole nitrogen donor atoms.

Hence, for the μ-oxo dimers with para-substituted phenyl groups, the increase in $|J|$ seen both in the solid state (Table I) and in solution (Table II) with increasing electron-donating ability of the substituents can be related to the resultant larger electron density on the pyrrole nitrogens. Electronic interactions between the iron atomic orbitals and the electron density in the porphyrin molecular orbitals centered on the pyrrole nitrogens would be expected to result in core expansion. The consequent decrease in bonding interactions between iron and the equatorial nitrogen ligands and increase in attraction for the axial oxo ligand would be reflected in decreased axial bond distance and stronger antiferromagnetic coupling through the oxo ligand.

$[(TPP(F_5))Fe]_2O$ was included in the study as an example of a highly electron-withdrawing substituent on the basis of the reported redox behavior of the free base.[5] However, existence of a monomeric hydroxo complex under appropriate conditions[25] indicates considerable steric hindrance between the *o*-fluorine substituents and suggests that the pentafluorophenyl compound cannot be regarded simply as an extension of the series of para-substituted tetraphenylporphinato ligands. Because of the unfavorable steric interactions, the significant difference between the solid-state and solution magnetic properties is not surprising. Although the solution measurements are consistent with predicted trends for a highly electron-withdrawing substituent, the marked decrease in C_t–N and $|J|$ could result from doming and rapid equilibration with high-spin monomers. A crystal structure would be helpful in interpreting the solid-state data, and efforts are currently in progress to obtain crystals suitable for structural determination by single-crystal X-ray diffraction.

Acknowledgment. This work was supported by the National Science Foundation through Grant No. CHE 83 08129 and by USPHS Grant No. ES 03433.

Registry No. $[(TPP)Fe]_2O$, 12582-61-5; $[(TPP(4\text{-}OCH_3))Fe]_2O$, 37191-17-6; $[(TPP(4\text{-}CF_3))Fe]_2O$, 101954-96-5; $[(TPP(F_5))Fe]_2O$, 81245-20-7; [(TPP)Fe]Cl, 16456-81-8; $[(TPP(4\text{-}OCH_3))Fe]Cl$, 19496-18-5; $[(TPP(4\text{-}CF_3))Fe]Cl$, 101954-97-6; $[(TPP(F_5))Fe]Cl$, 36965-71-6.

Supplementary Material Available: Table SI, temperature-dependent carbon-13 chemical shifts for pyrrole α- and β-carbon atoms, and Figures S1–S3, plots of magnetic moments vs. temperature (5 pages). Ordering information is given on any current masthead page.

(24) Hoffman, A. B.; Collins, D. M.; Day, V. W.; Fleischer, E. B.; Srivastava, T. S.; Hoard, J. L. *J. Am. Chem. Soc.* **1972**, *94*, 3620.

(25) Chromatography of the μ-oxo dimer on neutral alumina with methylene chloride eluant yields a crystalline solid with the following properties: ^1H NMR (250 MHz, methylene-d_2 chloride), broad singlet, 81 ppm (pyrrole H); UV–vis (methylene chloride), λ_{max} 405, 565 nm. Under these conditions there is no possibility of metathesis to the chloro complex; the UV–vis spectrum did not change after the ^1H NMR spectrum was recorded but reverted to that of the μ-oxo dimer when the solution was allowed to stand.